Dalton Transactions

Cite this: *Dalton Trans.*, 2012, **41**, 432

www.rsc.org/dalton

PAPER

Heterometallic platinum(II) compounds with β-aminoethylferrocenes: synthesis, electrochemical behaviour and anticancer activity†

Daniel Nieto,[a] Ana M. González-Vadillo,*[a] Sonia Bruña,[a] César J. Pastor,[b] Carla Ríos-Luci,[c] Leticia G. León,[c] José M. Padrón,[c] Carmen Navarro-Ranninger[a] and Isabel Cuadrado*[a]

Received 19th July 2011, Accepted 14th September 2011
DOI: 10.1039/c1dt11358e

A new family of heterometallic compounds **3–6** containing ferrocenyl and platinum(II) centers has been synthesized by reaction of 1-β-aminoethylferrocene (**1**) and 1,1′-bis(β-aminoethyl)ferrocene (**2**) with Pt(II) precursors. Using $K_2[PtCl_4]$ as the Pt(II) source, the *cis*-square-planar neutral compounds $[Fe\{\eta^5\text{-}C_5H_4(CH_2)_2NH_2\}_2PtCl_2]$ (**3**) and $[\{Fe(\eta^5\text{-}C_5H_4(CH_2)_2NH_2)(\eta^5\text{-}C_5H_5)\}_2PtCl_2]$ (**5**) were obtained. Reaction of *cis*-$[PtCl_2(dmso)_2]$ with **1** and **2** resulted in the displacement of dmso and chloride ligands from the platinum coordination sphere, affording the cationic and neutral compounds $[Fe\{\eta^5\text{-}C_5H_4(CH_2)_2NH_2\}_2Pt(dmso)Cl]Cl$ (**4**) and $[Fe(\eta^5\text{-}C_5H_4(CH_2)_2NH_2)(\eta^5\text{-}C_5H_5)Pt(dmso)Cl_2]$ (**6**). Compounds **3–6** were thoroughly characterized using multinuclear (^1H, ^{13}C, ^{195}Pt) NMR, IR spectroscopy, ESI mass spectrometry and elemental analysis. Single-crystal X-ray analysis of heterometallic **6** confirmed the *cis* geometry of the molecule and revealed that the platinum atom is held in a perfect square-planar geometry. The electrochemical behaviour of the heterometallic compounds **3–6**, which has been examined by cyclic (CV) and square wave (SWV) voltammetries in dichloromethane and dmso solution, is characterized by the reversible one-electron oxidation of the ferrocene moieties. The results of the biological activity studies revealed that the organometallic complex **5** is active against all cell lines with GI_{50} values in the range 1.7–2.3 μM. When compared to the standard anticancer drug cisplatin, heterotrimetallic **5**, possessing two aminoethylferrocenyl units coordinated to the Pt(II) center, showed a greater activity profile in the colon cancer cell line. Cell cycle studies revealed that the new mixed compound exhibits a mechanism of action different to cisplatin.

Introduction

Ferrocene derivatives possessing reactive functionalities tethered to the cyclopentadienyl rings have been extensively used to synthesize a broad variety of ferrocenyl-containing molecules with interesting applications, ranging from homogeneous catalysis to molecular recognition and materials science.[1] Among these metallocenes, amino-functionalized ferrocenes[2,3] are an attractive group of compounds that play a significant role in areas such as asymmetric catalysis, NLO materials, and coupling with biomolecules.[1] Furthermore, several amino-functionalized ferrocenes have been investigated as electroactive sensors of anions[4] in the modification of electrode surfaces,[5] as redox mediators in electrochemical biosensing of DNA and proteins,[6] and as ancillary ligands (with Pd and Pt centers) for olefin polymerizations.[7] An interesting recent report has shown that 1,1′-bis(amino)ferrocenes are also useful as starting compounds for gadolinium(III)-containing macrocyclic DPTA systems employed as MRI blood-pool contrast agents.[8]

Among aminoferrocenes, mono and bisfunctionalized β-aminoethylferrocenes $Fe\{(\eta^5\text{-}C_5H_4(CH_2)_2NH_2)(\eta^5\text{-}C_5H_5)\}$ (**1**) and $Fe\{\eta^5\text{-}C_5H_4(CH_2)_2NH_2\}_2$ (**2**) (Chart 1) are particularly interesting compounds since they are able to undergo condensation reactions typical of the primary amino functional group. Pioneering studies in this field were carried out by Gonsalves and Rausch, who have used 1,1′-bis(β-aminoethyl)ferrocene (**2**) as starting monomer for the preparation of remarkable examples of ferrocene-containing polyamides and polyureas (see example in Chart 1) *via* interfacial condensation polymerizations.[9] Likewise, our group has also used aminoethyl ferrocenes **1** and **2** as useful precursors of silicon-containing ferrocenyl model compound polymers (Chart 1).[10]

The high reactivity of the primary amine group of monofunctionalized 1-β-aminoethylferrocene (**1**) toward Si–Cl bonds also

[a]*Departamento de Química Inorgánica, Facultad de Ciencias, Universidad Autónoma de Madrid, Cantoblanco, 29049, Madrid, Spain. E-mail: anam.gonzalez@uam.es, isabel.cuadrado@uam.es; Fax: +34 91 497 4833; +34 91 497 4843; +34 91 497 4834*
[b]*Laboratorio de Difracción de Rayos X, SIDI, Universidad Autónoma de Madrid, Spain*
[c]*BioLab, Instituto Universitario de Bio-Orgánica "Antonio González" (IUBO-AG). Universidad de La Laguna, 38206, La Laguna, Spain*

† Electronic supplementary information (ESI) available: Additional spectroscopic data for **1–6**; electrochemical details for **3–6** and crystallographic data for **6**. CCDC reference number 834095. For ESI and crystallographic data in CIF or other electronic format see DOI: 10.1039/c1dt11358e

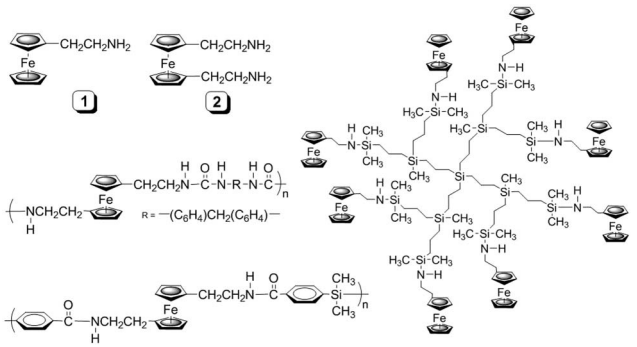

Chart 1 β-Aminoethylferrocene precursors **1** and **2** and selected polymer and dendrimer derivatives.

allowed facile organometallic functionalization of carbosilane frameworks, resulting in dendrimers with 4 and 8 ferrocenyl moieties attached to the surface of the dendritic structure through Si–NH linkages (see example in Chart 1).[11] These ferrocenyl dendrimers are able to act as anion receptors, in solution and immobilized onto electrode surfaces.[12] Surprisingly, and although β-aminoethylferrocenes **1** and **2** are also valuable building blocks for coordination compounds of higher nuclearity, their coordination chemistry remains largely unexplored. To our knowledge, only a few examples of cyclometallated Pd(II) and Pt(II) compounds derived from **1** have been reported.[13]

On the other hand, derivatives based on typical organometallic moieties such as ferrocene, titanocene dichloride, and arene ruthenium units have been extensively investigated in recent years as a novel class of medicinal compounds, potentially with new metal-specific modes of action.[14,15] In particular, a number of simple neutral ferrocene derivatives as well as some cationic ferrocenium salts exhibit cytotoxic behaviour and inhibit the development of tumors *in vivo*.[15–16] In addition, the ferrocene unit has also been linked to platinum,[17] palladium or ruthenium centers in order to achieve synergistic biological effects between the two active metals.[18,19]

As part of our longstanding interest in the chemistry of ferrocenyl-containing compounds and dendrimers[20,21] and in the preparation and study of platinum-based derivatives with antitumoral properties,[22] we recently became interested in using β-aminoethylferrocenes **1** and **2** for the synthesis of new series of potentially cytotoxic heterometallic ferrocene-containing Pt(II) and Pt(IV) complexes. In this context, we have recently found that the reaction of **1** with the platinum(II) benzonitrile complex *cis*-[$PtCl_2(PhCN)_2$] affords an interesting compound, *trans*-[$PtCl_2\{NH{=}C(Ph)(NH(CH_2)_2Fc)\}_2$] having newly formed ferrocenyl-amidine ligands, which is able to act as an electrochemical sensor for the $H_2PO_4^-$ anion.[23]

Herein, we report on the reactivity of β-aminoethylferrocenes **1** and **2** towards $K_2[PtCl_4]$ and *cis*-[$PtCl_2(dmso)_2$] complexes as platinum(II)-containing sources, which has led to the isolation of new electroactive heterometallic platinum-based compounds. Their complete structural characterization and redox behaviour are described, along with their cytotoxic activity against a panel of human solid tumor cell lines containing examples of HBL-100 (breast), HeLa (cervix), SW1573 (non-small cell lung), and WiDr (colon).

Results and discussion

Synthesis and characterization of β-aminoethylferrocenes

The starting ferrocenyl derivatives required for the present study were 1-β-aminoethylferrocene (**1**) and 1,1′-bis(β-aminoethyl)-ferrocene (**2**). These compounds in particular were selected since their reactive NH_2 functionalities are separated from the cyclopentadienyl ring by a two methylene flexible spacer. This fact is of importance because it minimizes steric and electronic effects of the organometallic ferrocene moiety. The use of a β-functionalized metallocene, in addition, avoids the instability of α-functional ferrocene derivatives resulting from the stability of the α-ferrocenyl carbonium ion.[24] Both aminoethylferrocenes, **1** and **2**, were synthesized several decades ago,[25,26] but slightly modified preparations were used here to improve yields and to ease purification. Scheme 1 summarizes the sequence of multiple reaction steps to give **1** and **2** (Scheme 1, top and bottom, respectively).

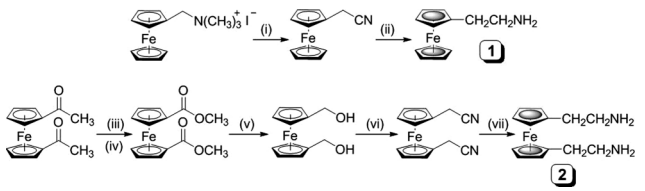

Scheme 1 Reagents and conditions for the synthesis of β-aminoethylferrocenes **1** and **2**. (i) KCN, H_2O, reflux; (ii) $LiAlH_4$, Et_2O, reflux; (iii) NaOCl, 50 °C; (iv) CH_3OH, H_2SO_4, 90 °C; (v) $LiAlH_4$, Et_2O/toluene (1/1, v/v), reflux; (vi) Py, PCl_3, KCN, THF/H_2O, 40 °C; (vii) $LiAlH_4$, $AlCl_3$, Et_2O, reflux.

Monofunctionalized β-aminoethylferrocene (**1**) was prepared in two steps (i and ii, in Scheme 1, top) from *N*,*N*,*N*-trimethylferrocenylmethyl-ammonium iodide as starting material by adapting the literature procedures. Firstly, $[(\eta^5\text{-}C_5H_5)Fe\{(\eta^5\text{-}C_5H_4)CH_2N(CH_3)_3\}]I$ was reacted with potassium cyanide, thus resulting in 1-cyanomethylferrrocene which was isolated as a yellow crystalline solid in 63% yield. The cyanomethylferrocene was converted into β-aminoethylferrocene (**1**) by reduction with $LiAlH_4$ followed by treatment with aqueous sodium hydroxide. After aqueous workup and distillation in vacuum, primary amine **1** was obtained as an amber-brown oil in 66% yield.

For the synthesis of bifunctionalized ferrocenyl derivative **2** (Scheme 1, bottom), 1,1′-ferrocenyldicarboxylic acid was firstly prepared on a large scale by oxidation of 1,1′-diacetylferrocene with sodium hypochlorite. After purification, dicarboxyferrocene was converted into the corresponding dimethyl ester by acid-catalyzed esterification (Scheme 1, step iv). Subsequent reduction of the methyl diester with $LiAlH_4$ (Scheme 1, step v) afforded 1,1′-bis(β-hydroxymethyl)ferrocene. This diol was converted into the nitrile and its subsequent reduction with $LiAlH_4$ produced the desired amine **2** (steps vi and vii in Scheme 1).

As only a few structural characterization data of **1** and **2** have been previously reported, a detailed characterization of both aminoethylferrocenes was accomplished by NMR spectroscopy, including $\{^1H\text{–}^{13}C\}$HMQC and $\{^1H\text{–}^{13}C\}$HMBC experiments, IR spectroscopy, and mass spectrometry (see ESI). ^1H and ^{13}C NMR spectra of **1** and **2** showed the shifts for the CH_2 groups

bonded to the nitrogen atom at a higher δ (ppm) than those for the other CH_2 groups. While the ^1H NMR spectrum of **2** shows the typical patterns of disubstituted ferrocene derivatives, two pseudo-triplets, the ^1H NMR spectrum of **1** shows the characteristic pattern for monosubstituted ferrocenes, two pseudo-triplets and a singlet. The amine group protons of both compounds appear at about 1.3 ppm, which was proved by the disappearance of the signals when some D_2O drops were added to the NMR sample. The most relevant feature of the IR spectra of ferrocenylamines **1** and **2** consists of the presence of bands, in the range of 3292–3368 cm^{-1} due to the N–H stretching vibrations. The ESI mass spectra show a peak corresponding to the M^+ ion, at m/z 229 (for **1**) and at 272 (for **2**), together with some peaks assignable to reasonable fragmentation products.

Reactivity of β-aminoethylferrocenes 1 and 2 with $K_2[PtCl_4]$ and *cis*-$[PtCl_2(dmso)_2]$ complexes

Our initial attempts to prepare mixed platinum(II)-aminoethylferrocene compounds involved the use of the salt $K_2[PtCl_4]$ as the platinum(II)-containing source. The β-aminoethylferrocene precursors **1** and **2** were soluble in dichloromethane, whereas this platinum starting material was not. For this reason, the heterometallic complexes, *cis*-dichloro[1,1′-bis(β-aminoethyl)ferrocene]platinum(II) (**3**) and *cis*-dichlorobis[1-β-aminoethylferrocene]platinum(II) (**5**) were prepared using a biphasic system with the aminoethylferrocenes **1** and **2** in a CH_2Cl_2 solution and the platinum starting salt dissolved in an ethanol–water mixture. The use of this synthetic route avoids the difficulties related to the basicity of ferrocenylamines in aqueous solution that could lead to the formation of ferrocenylamine salts. The reaction mixture was stirred vigorously at room temperature to increase the interface of reaction between the solvent layers. A phase-transfer reaction was established between the layers. The heterometallic products were found to be soluble in the dichloromethane phase. After appropriate work-up, compounds **3** and **5** (Scheme 2) were obtained in reasonable yields as yellow-orange crystalline solids.

On the other hand, when *cis*-$[PtCl_2(dmso)_2]$ was reacted with **2** in dichloromethane solution, a yellow solid product was obtained which was identified as $[Fe\{\eta^5\text{-}C_5H_4(CH_2)_2NH_2\}_2Pt(dmso)Cl]Cl$ (**4**) (Scheme 2). Analogous reaction of *cis*-$[PtCl_2(dmso)_2]$ with mono-functionalized ferrocene **1** in the same medium afforded, after appropriate column chromatographic purification, a yellow shiny solid whose characterization data (see below and ESI†) agreed with those expected for the dimetallic compound $[Fe(\eta^5\text{-}C_5H_4(CH_2)_2NH_2)(\eta^5\text{-}C_5H_5)Pt(dmso)Cl_2]$ (**6**). Coordination of β-aminoethylferrocenes to platinum centers resulted in the displacement of one dmso and one chloride ligand from the coordination sphere of platinum, leading to the cationic compound **4**, or one dmso ligand yielding neutral bimetallic **6**. This reactivity is different to that found by Lopez *et al.* in the reactions of ferrocenylamine **1** with palladium(II) complexes, in which cyclopalladation of the β-aminoethylferrocene **1** was observed, as a result of the coordination of the nitrogen atom of **1** to palladium followed by intramolecular electrophilic attack to the σ C–H bond of the cyclopentadienyl ring.[13a]

The structural identity of the novel molecules **3–6** was straightforwardly established on the basis of elemental analysis, IR, multinuclear (^1H, ^{13}C, ^{195}Pt) NMR spectroscopy and mass spectrometry, when it was possible. Although the poor solubility of compound **3** in common organic solvents precluded any reasonable NMR analyses (^1H and ^{13}C NMR), its structure was confirmed by ESI mass spectrometry. The ion $[M–Cl]^+$ was clearly observed at m/z 501.0 and its calculated and experimental isotopic distributions are in total agreement. Furthermore, the IR spectrum of **3** (in KBr) agrees well with the proposed structure, as it exhibits a band at 487 cm^{-1} due to the Pt–N stretching vibration, and two bands due to the stretching of the Pt–Cl bonds (at 330 and 321 cm^{-1}) indicative of the *cis* geometry.[27]

Compounds **4**, **5** and **6** proved to be much more soluble in common organic solvents than compound **3**, so further characterization could be achieved by NMR spectroscopy. While proton NMR spectra of **5** (in dmso-d_6) and **6** (in CD_2Cl_2) show the typical patterns of monosubstituted ferrocene derivatives (a singlet for the C_5H_5 protons, and two pseudo-triplets for the C_5H_4 moiety, which in **6** are under the singlet signal), the ^1H NMR spectrum of **4**, in $(CD_3)_2CO$, shows two signals at 4.19 and 4.12 ppm, typical of disubstituted ferrocene derivatives. The expected signals for the protons of the CH_2 groups (**4–6**) appear at higher ppm than the same protons of the precursors **1** and **2**. In addition, an intense singlet, at 3.34 (for **4**) and at 3.44 (for **6**), assigned to the protons of the dmso ligands, can be observed. In particular, the proton NMR spectra of **4** and **6** display ^{195}Pt satellites for this last resonance with $^3J(^{195}Pt–^1H) = 19.1$ Hz (**4**) and 25.5 Hz (**6**). A remarkable ^1H NMR feature of **4–6** is the chemical shift of the NH groups of the amine ligands, as they are considerably shifted downfield (at 4.50 for **4**,

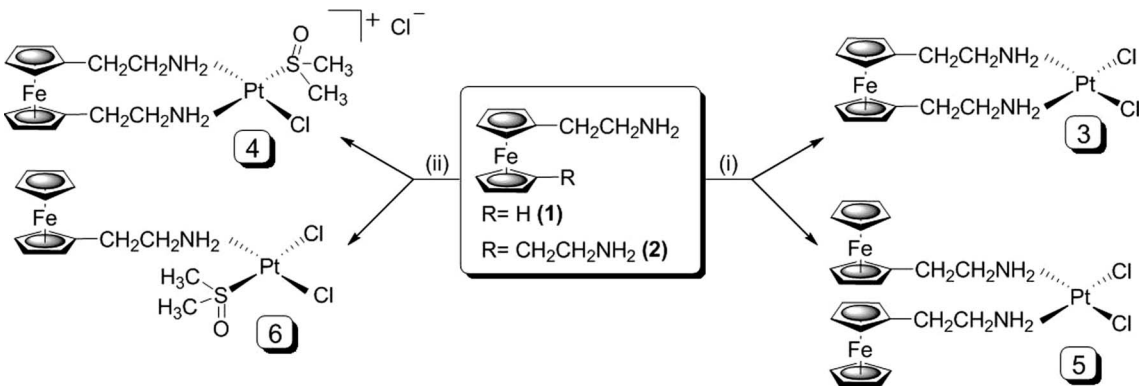

Scheme 2 Synthesis of heterometallic compounds **3–6**. Reagents and conditions: (i) $K_2[PtCl_4]$, H_2O/EtOH (2/1, v/v), CH_2Cl_2; (ii) *cis*-$[PtCl_2(dmso)_2]$, CH_2Cl_2, r.t.

4.98 for **5**, and 3.82 for **6**) in comparison with the signals of the free ligands of **1** (1.30 ppm) and **2** (1.24 ppm).

The ^{195}Pt resonance is extremely sensitive to the coordination environment, so the ^{195}Pt{H} NMR spectra of compounds **4–6** provide convincing evidence for the coordination sphere and structure of the mixed ferrocene and platinum complexes. While the signal detected in the ^{195}Pt{H} NMR spectrum of compound **4** (in $(CD_3)_2CO$) appears at −3120 ppm and for **6** (in CD_2Cl_2) at −3097 ppm, for compound **5** (in dmso-d_6) the signal is shifted downfield (−2210 ppm). These values are consistent with a N_2ClS,[28] NCl_2S[29] and N_2Cl_2,[22b] set of donor atoms around the platinum center, respectively.

The IR spectra of **3** and **5** (KBr) show two bands due to the stretching of the Pt–Cl bond, according to a *cis* structure, and one band due to the Pt–N stretching vibration. For **4** and **6**, in addition to the latter signals (see experimental section) the typical bands due to the presence of dmso are observed. Namely ν(S═O) appears at 1124 cm^{-1} for **4** and at 1123 cm^{-1} for **6**, and ν(Pt–S) at 441 cm^{-1} for **4** and at 444 cm^{-1} for **6**.

The mass spectrometric studies of compounds **4–6** have provided further support for the existence of the heterometallic compounds. In the ESI-MS spectrum of trimetallic **5** a peak at *m*/*z* 723.0 corresponding to the molecular ion $[M]^+$ was observed. In addition, the spectrum exhibits a peak corresponding to the cationic fragment $[M–Cl]^+$ (at 688.0), due to the loss of Cl^-. Their isotopic distributions are in excellent agreement with the calculated ones. Mass spectral analysis (ESI) of **4** and **6** confirmed the proposed structures, showing the corresponding molecular ions $[M]^+$ at *m*/*z* 580.0 (for **4**), and $[M+Na]^+$ at *m*/*z* 594.9 (for **6**), as the most intense signals, with an excellent agreement between the calculated and the found isotopic patterns (see Fig. S13 and S23, ESI†).

In order to confirm the relative arrangement of the ferrocenyl, chloride and dmso ligands in heterometallics **3–6**, several crystallization procedures were used; however, most of the experiments failed. Only when a hexane/CH_2Cl_2 solution of **6** was evaporated at +4 °C suitable crystals were obtained. The molecular structure of the platinum complex **6** together with the atomic numbering scheme is shown in Fig. 1. Crystallographic data are shown in Table 1 while selected bond lengths and angles are shown in Table 2.

Heterobimetallic **6** crystallizes in the monoclinic $P2_1/c$ space group with $Z = 4$. The coordination environment of the platinum ion is square planar, with two *cis* chloride ligands, one nitrogen atom of the ferrocenylamine and one sulfur atom of the dmso unit. Consequently, *cis* bond angles around the Pt center are very close to the expected 90°, and S(1)–Pt(1)–Cl(1) and N(1)–Pt(1)–Cl(2) angles have values of 175–176°. Moreover, the compound exhibits two hydrogen bonds, one of them intramolecular between the N(1)–H(1A) proton of the amine and the oxygen atom O(1), and the other intermolecular between the N(1)–H(1B) proton and the chlorine atom Cl(2) of another molecule with bond distances of 2.24 and 2.86 Å, respectively.

The Pt–S length (S(1)–Pt(1) 2.199(2) Å) is similar to those reported for other Pt–sulfoxide complexes with a chlorine in the *trans* position.[30,31] The Pt–Cl bond *trans* to the sulfoxide ligand is longer (2.324(2) Å) than the one *trans* to the amine (2.294(19) Å). This elongation of the Pt–Cl(1) distance confirms the major *trans* effect of the sulfur donor atom.

Table 1 Selected crystallographic data for compound **6**

6	
Empirical formula	$C_{14}H_{21}Cl_2FeNOPtS$
Fw	573.22
T [K]	100(2)
λ [Å]	1.54178
cryst syst	Monoclinic
Space group	$P2_1/c$
a, Å	13.1200(12)
b, Å	11.3110(10)
α, deg	11.8689(10)
β, deg	90
c, Å	97.208(5)
γ, deg	90
V, Å^3	1747.4(3)
Z	4
density (calcd), mgm^{-3}	2.179
μ, mm^{-1}	25.317
F(000)	1096
Crystal size, mm^3	0.20 × 0.14 × 0.08
θ, deg	3.40 to 68.26.
Index ranges	$-14 \le h \le 15$ $-12 \le k \le 13$ $-13 \le l \le 13$
no. of reflns collected	13 604
no. of indep reflns	3017 [R(int) = 0.0572]
completeness	94.2% (to θ = 68.26°)
absorp corr	semi-empirical from equivalents
refinement method	full-matrix least-squares on *F*2
no. of data/restraints/params	3017/0/180
goodness-of-fit on *F*2	1.048
Final *R* indices ($I > 2\sigma(I)$)	$R_1 = 0.0431$, w$R_2 = 0.0984$
R indices (all data)	$R_1 = 0.0486$, w$R_2 = 0.1026$
largest diff peak and hole/e Å^{-3})	4.028 and −2.078

Table 2 Selected bond lengths (Å) and angles (°) for compound **6**

6			
Pt(1)–Cl(1)	2.324(2)	Cl(1)–Pt(1)–S(1)	176.5(8)
Pt(1)–Cl(2)	2.294(19)	N(1)–Pt(1)–Cl(2)	175.1(2)
Pt(1)–N(1)	2.089(8)	N(1)–Pt(1)–S(1)	89.9(2)
Pt(1)–S(1)	2.199(2)	Cl(1)–Pt(1)–Cl(2)	90.8(8)
Pt(1)–Fe(1)	7.002	S(1)–Pt(1)–Cl(2)	92.2(8)
S(1)–O(1)	1.465(6)	N(1)–Pt(1)–Cl(1)	87.2(2)
S(1)–C(1)	1.764(9)	Pt(1)–S(1)–O(1)	114.4(3)
S(1)–C(2)	1.767(10)	Pt(1)–S(1)–C(1)	112.7(3)
N(1)–C(3)	1.443(13)	Pt(1)–S(1)–C(2)	110.1(3)
N(1)–H(1A)	0.920	C(1)–S(1)–C(2)	101.5(4)
N(2)–H(1B)	0.920	Pt(1)–N(1)–C(3)	111.1(6)
C(3)–C(4)	1.550(14)	C(3)–C(4)–C(5)	112.6(9)
C(4)–C(5)	1.491(14)		

The S atom in the dmso ligand is in an approximately tetrahedral environment. The Pt(1)–S(1)–O(1) angle (114.4(3)°) is slightly larger than the Pt(1)–S(1)–C(1) and Pt(1)–S(1)–C(2) angles (112.7(3) and 110.1(3)°, respectively) and the C(1)–S(1)–C(2) angle (101.5(4)°) is smaller than the other angles around the S atom, since the multiple S–O bond occupies more space than the single S–C bonds.

In the ferrocenyl moiety, the two cyclopentadienyl rings are essentially parallel and they are arranged, approximately, in a nearly eclipsed conformation. The distance between the two metals in the molecule (Fe···Pt) is 7.002 Å.

The molecular arrangement of **6** in the crystal structure shown in Fig. 2 is of interest. An examination of the crystal packing diagram along the *b*-axis shows that association of similar metallic

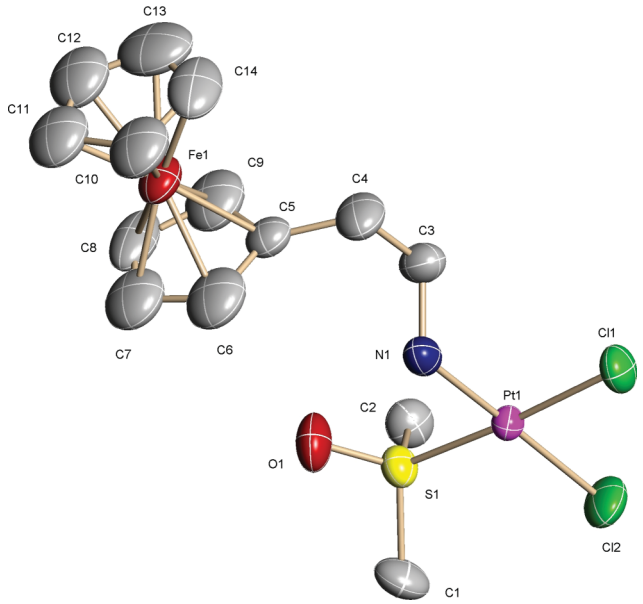

Fig. 1 Molecular structure of **6** with 50% probability ellipsoids. Hydrogen atoms are omitted for clarity.

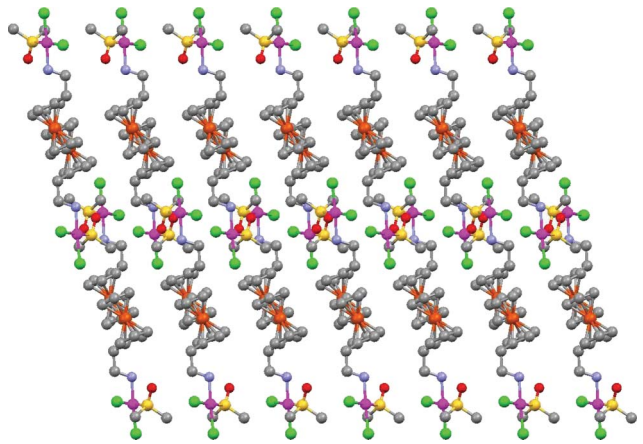

Fig. 2 Crystal-packing diagram of trimetallic **6** along the *b*-axis, showing the iron-rich and platinum-rich pseudolayers.

moieties, a type of self-assembly, is apparently driving the packing in the crystal. The intermolecular ferrocene distances to the next neighboring molecules range between 5.967 and 6.245 Å, placing the metallocene moieties in a favorable proximity for cluster-forming intermolecular solid-state reactions. Thus, one can clearly observe repeating platinum-rich and ferrocenyl-rich layers lying in the *ac*-plane.

Electrochemical studies

The anodic electrochemistry of the heterometallic compounds **3**–**6** was examined by cyclic voltammetry (CV) and square wave voltammetry (SWV), using dichloromethane or dmso as solvents, and tetra-*n*-butylammonium hexafluorophosphate (*n*-Bu_4NPF_6) as the supporting electrolyte. The low solubility of **3** did not allow us to carry out electrochemical studies in the non-nucleophilic solvent dichloromethane.

The cyclic voltammograms of heterometallic compounds **3**, **4** and **6** in dmso, in the anodic potential region between 0 and +1 V *vs.* SCE, exhibit a single oxidation about +0.45 V, assigned to the Fe^{2+}/Fe^{3+} redox system. Representative CVs and SWVs are given in Fig. 3 (for compounds **5** and **6**) as well as in the ESI.† In all cases, the linearity of i *vs.* $v^{1/2}$ plots (see ESI†) demonstrates that the main mass transport of these compounds to the electrode surface is controlled by the diffusion step. Likewise, the voltammetric features (i_{pc}/i_{pa} essentially equal to unity, ΔE_{peak} values about 60–85 mV and E_{peak} independent of the scan rate) show that oxidation of these mixed ferrocene–platinum compounds is chemically and electrochemically reversible, resulting in the production of stable and soluble species **[3⁺][PF₆⁻]**, **[4⁺][PF₆⁻]** and **[6⁺][PF₆⁻]**.

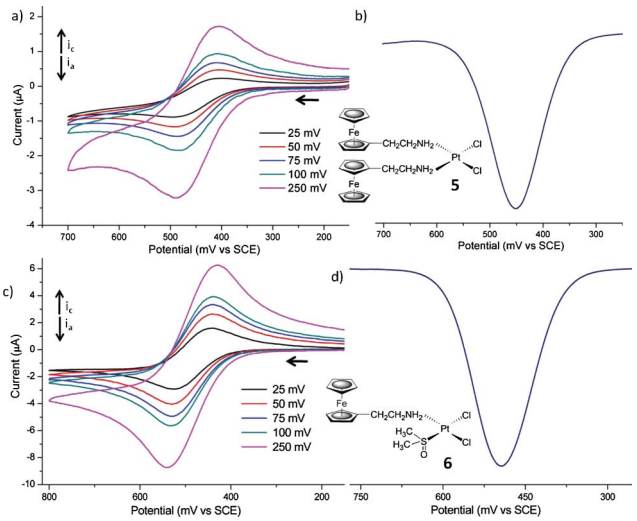

Fig. 3 CV (at different scan rates) and SWV responses of compounds **5** in dmso (a and b) and **6** in CH_2Cl_2 (c and d) (5×10^{-4} M) on platinum working electrode (nominal area 0.020 cm^2).

The electrochemical behaviour of heterotrimetallic **5**, containing two ferrocenyl moieties and one platinum(II) center, in dmso solution, is reversible and shows a single oxidation peak at $E_{1/2}$ = 0.45, *vs.* SCE (see Fig. 3a) suggesting the formation of the stable and soluble cationic species **[5²⁺][PF₆⁻]₂**. Likewise, in the square wave voltammogram (Fig. 3b) only one oxidation wave is observed. The fact that only a single redox process is observed implies simultaneous two-electron transfers at the same potential as the ferrocenyl units in **5**, indicating the lack of electronic communication between the two ferrocenyl centers.[32]

Antiproliferative activity

As a model for anticancer activity we used the human solid tumor cell lines HBL-100 (breast), HeLa (cervix), SW1573 (non-small cell lung), and WiDr (colon). The *in vitro* antiproliferative activity of complexes **4**–**6** was evaluated after 48 h of drug exposure using the sulforhodamine B (SRB) assay.[33] Compound **3** was not soluble enough in dmso (40 mM) to proceed with biological experiments. The results expressed as GI_{50} (50% growth inhibition)[34] values are shown in Table 3.

For comparison, we have included the antiproliferative data of the standard anticancer drug cisplatin (CDDP) against the same panel of solid tumor cell lines. The data shows that the organometallic complex **5**, with two aminoethylferrocenyl units coordinated to the Pt(II) center, was the most potent compound

Table 3 *In vitro* antiproliferative activity against human solid tumor cells[a]

Compound	Cell line (type)			
	HBL-100 (breast)	HeLa (cervix)	SW1573 (lung)	WiDr (colon)
4	>100	>100	>100	>100
5	2.0 (±0.49)	1.7 (±0.19)	2.0 (±0.71)	2.3 (±0.52)
6	32 (±0.74)	27 (±7.4)	30 (±3.4)	41 (±13)
CDDP	1.9 (±0.16)	2.0 (±0.3)	3.4 (±0.7)	26 (±5.6)

[a] Values expressed as GI_{50} are given in μM and are means of two to six experiments, standard deviation is given in parentheses.

of the series with GI_{50} values in the range 1.7–2.3 μM. In contrast, compound **6** showed reduced activities while complex **4** was inactive. When compared to cisplatin, compound **5** showed a superior activity profile in the more drug resistant[35] cell line WiDr. Compound **5** was selected as a lead for further biological evaluation.

Cell cycle studies

To investigate the effects that the mixed ferrocene–platinum complex **5** produces on tumor cells and to highlight possible differences in its mode of action, cell cycle analysis[36] by flow cytometry was performed on the cancer cell lines HeLa, SW1573, and WiDr after 24 h exposure to the drugs. The standard anticancer drug cisplatin was used as a reference drug to compare the results. Cells were exposed to each agent at two drug concentrations that were chosen based on two premises:[37] the GI_{50} values of the compounds and the sensitivity of the cell line to drug treatment, since at higher drug doses cell death prevents examination of the cell cycle phase distribution. Thus, all cell lines were initially exposed for 24 h to compound **5** at 2 and 6 μM drug doses and to cisplatin at 5 and 10 μM. The obtained results showed that the cell cycle in all cell lines was little affected at the low dose of 2 μM. No clear cell cycle arrest could be observed even at the higher dose of 6 μM (Fig. 4). However, only HeLa cells showed significant cell death (12%), similar to cisplatin (13% at 5 μM). Increasing the dose to 18 μM only produced significant cell death in SW1573 cells (12%), while changes in the cell cycle of HBL-100 cells were irrelevant. In contrast, cisplatin produces a clear S-phase arrest, even at higher doses. The results indicate that the mechanism of antiproliferative activity of the new compound is not affecting the cell cycle.

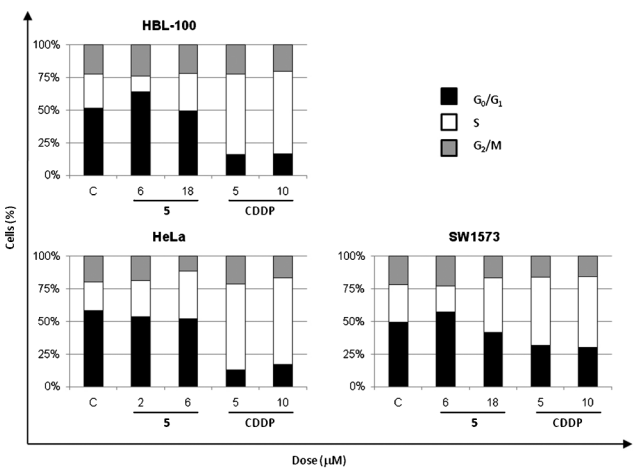

Fig. 4 Cell cycle phase distribution of untreated cells (C) and cells treated (drug dose in μM) with complex **5** and cisplatin (CDDP) for 24 h.

The combination of the ferrocene and the diamino-platinum scaffolds indicates a possible role of the ferrocene moiety in the modulation of the antiproliferative activity of the diamino-platinum framework. Ongoing studies beyond the scope of this work will help to establish the precise role of both active functions and any possible synergistic interaction.

Experimental

Materials and equipment

All reactions and compound manipulations were performed in an oxygen- and moisture-free atmosphere (N_2 or Ar) using standard Schlenk techniques. Solvents were dried by standard procedures over the appropriate drying agents and distilled immediately prior to use. The platinum precursor *cis*-[$PtCl_2(dmso)_2$] was prepared by literature methods.[38] 1,1′-Diacetylferrocene, methanol, sodium hypochlorite solution 5% (Aldrich), potassium cyanide, aluminum chloride (Fluka), potassium tetrachloroplatinate(II), *N*,*N*,*N*-trimethylferrocenylmethyl-ammonium iodide and lithium aluminum hydride (Alfa Aesar) were used without further purification. Phosphorus trichloride and pyridine (Aldrich) were distilled prior to use. Silica gel 60 silanized (Merck) was used for column chromatographic purifications. Infrared spectra were recorded on Bomem MB-100 FT-IR and on Perkin Elmer 100 FT-IR spectrometers. ^1H, ^{13}C, ^{195}Pt NMR spectra, were recorded on Bruker-AMX-300 and Bruker-DRX-500 spectrometers. Chemical shifts were reported in parts per million (δ) with reference to residual solvent resonances for ^1H and ^{13}C NMR ($CDCl_3$: ^1H, δ 7.27 ppm, ^{13}C, δ 77.0 ppm; $(CD_3)_2CO$: ^1H, δ 2.09 ppm; ^{13}C, δ 205.9 and 30.6 ppm; dmso-d_6: ^1H, δ 2.54 ppm, ^{13}C, δ 40.45 ppm; and CD_2Cl_2: ^1H, δ 5.33 ppm, ^{13}C, δ 53.8 ppm). Electrospray ionization (ESI) mass spectra were recorded with a QSTAR (Applied Biosystems) spectrometer, using methanol as the ionizing phase, while FAB-mass spectra were obtained using a VG AutoSpec (Waters) mass spectrometer with *m*-NBA as the matrix. Samples were prepared in CH_2Cl_2 or dmso. Elemental analyses were performed by the Microanalytical Laboratory, SIDI, Universidad Autónoma de Madrid, Spain.

Electrochemical measurements

Cyclic voltammetric and square wave voltammetric experiments were recorded on a BAS-CV-50 W potentiostat. CH_2Cl_2 (dried over CaH_2) and dmso (spectrograde) for electrochemical measurements were freshly distilled under argon. The supporting

electrolyte used was tetra-*n*-butylammonium hexafluorophosphate (Fluka), which was purified twice by recrystallization from ethanol and dried in vacuum at 60 °C. The supporting electrolyte concentration was typically 0.1 M. A conventional three-electrode cell connected to an atmosphere of prepurified nitrogen was used. All cyclic voltammetric experiments were performed using either a platinum-disk working electrode (A = 0.020 cm^2) or a glassy carbon-disk working electrode (A = 0.070 cm^2) (both Bioanalytical Systems), each of which were polished on a Buehler polishing cloth with Metadi II diamond paste, rinsed thoroughly with purified water and acetone and dried. All potentials were referenced to the saturated calomel electrode (SCE). Under our conditions, the decamethylferrocene redox couple $[FeCp^*_2]^{0/+}$ is –0.06 V *vs.* SCE in CH_2Cl_2. A coiled platinum wire was used as a counter electrode. Solutions were typically 5×10^{-4} M in the redox active species. The solutions for the electrochemical experiments were purged with nitrogen and kept under an inert atmosphere throughout the measurements. Square wave voltammetry (SWV) was performed using frequencies of 10 Hz.

X-ray crystal structure determination

Compound **6** was structurally characterized by single-crystal X-ray diffraction. A suitable yellow crystal of **6**, of dimensions 0.20 × 0.14 × 0.08 mm, was located and mounted on a glass fiber with "magic oil". The sample was transferred to a Bruker SMART 6 K CCD area-detector three-circle diffractometer with a MacScience rotating anode (Cu-Kα radiation, λ = 1.54178 Å) generator equipped with Goebel mirrors at settings of 50 kV and 100 mA. A total of 3017 independent reflections (R_{int} = 0.0572) were colleted in the range $3.40° < \theta < 68.26°$. X-ray data were collected at 100 K, with a combination of six runs at different φ and 2θ angles, 3600 frames. Data were collected using 0.3° wide ω scans with a crystal-to-detector distance of 4.0 cm. The substantial redundancy in data allows empirical absorption corrections (SADABS)[39] to be applied using multiple measurements of symmetry-equivalent reflections. Raw intensity data frames were integrated with the SAINT program,[40] which also applied corrections for Lorentz and polarization effects. The software package SHELXTL version 6.10 was used for space group determination, structure solution and refinement.[41] The space group determination was based on a check of the Laue symmetry and systematic absences and was confirmed using the structure solution. The structure was solved by direct methods (SHELXS-97), completed with difference Fourier syntheses, and refined with full-matrix least-squares using SHELXL-97 minimizing $w(F_o^2–F_c^2)^2$.[42,43] Weighted R factors (R_w) and all goodness of fit S are based on F^2 conventional R factors (R) are based on F. All non-hydrogen atoms were refined with anisotropic displacement parameters. The hydrogen atom positions were calculated geometrically and were allowed to ride on their parent carbon atoms with fixed isotropic U. All scattering factors and anomalous dispersion factors are contained in the SHELXTL 6.10 program library.

Biology

All starting materials were commercially available research-grade chemicals and used without further purification. RPMI 1640 medium was purchased from Flow Laboratories (Irvine, UK), fetal calf serum (FCS) was from Gibco (Grand Island, NY), trichloroacetic acid (TCA) and glutamine were from Merck (Darmstadt, Germany), and penicillin G, streptomycin, dmso and sulforhodamine B (SRB) were from Sigma (St Louis, MO).

Cells, culture and plating

The human solid tumor cell lines HBL-100, HeLa, SW1573, and WiDr were used in this study. These cell lines were a kind gift from Prof. G. J. Peters (VU Medical Center, Amsterdam, The Netherlands). Cells were maintained in 25 cm^2 culture flasks in RPMI 1640 supplemented with 5% heat inactivated fetal calf serum and 2 mM L-glutamine in a 37 °C, 5% CO_2, 95% humidified air incubator. Exponentially growing cells were trypsinized and re-suspended in antibiotic containing medium (100 units penicillin G and 0.1 mg of streptomycin per mL). Single cell suspensions displaying >97% viability by trypan blue dye exclusion were subsequently counted. After counting, dilutions were made to give the appropriate cell densities for inoculation onto 96-well microtiter plates. Cells were inoculated in a volume of 100 mL per well at densities of 10 000 (SW1573 and HBL-100), 15 000 (HeLa), and 20 000 (WiDr) cells per well, based on their doubling times.

Chemosensitivity testing

Compounds were initially dissolved in dmso at 400 times the desired final maximum test concentration. Control cells were exposed to an equivalent concentration of dmso (0.25% v/v, negative control). Each agent was tested in triplicate at different dilutions in the range of 1–100 μM. The drug treatment was started on day 1 after plating. Drug incubation times were 48 h, after which time cells were precipitated with 25 μL ice-cold TCA (50% w/v) and fixed for 60 min at 4 °C. Then the SRB assay was performed.[33] The optical density (OD) of each well was measured at 492 nm, using BioTek's PowerWave XS Absorbance Microplate Reader. Values were corrected for background OD from wells only containing medium.

Cell cycle analysis

Cells were seeded in six well plates at a density of 2.5–5 × 10^5 cells well^{-1}. After 24 h the products were added to the respective well and incubated for an additional period of 24 h. Cells were trypsinized, harvested, transferred to test tubes (12 × 75 mm) and centrifuged at 1500 rpm for 10 min. The supernatant was discarded and the cell pellets were re-suspended in 200 μL of cold PBS and fixed by the addition of 1 mL ice-cold 70% EtOH. Fixed cells were incubated overnight at –20 °C, after which time they were centrifuged at 1500 rpm for 10 min. The cell pellets were resuspended in 500 μL of PBS and 5 μL of DNAse-free RNAse solution (10 mg mL^{-1}) was added. The mixture was incubated at 37 °C for 30 min. Finally, 5 μL of PI (0.5 mg mL^{-1}) was added. Flow cytometric determination of DNA content (20 000 cells sample^{-1}) was analyzed on a LRSII Flow Cytometer (Becton Dickinson, San José, CA, USA). The fractions of the cells in the G0/G1, S, and G2/M phases were analyzed using FACS Diva 6.0 (BD Software, San José, CA, USA) software.

Synthesis of Fe{[(η^5-C$_5$H$_4$)(CH$_2$)$_2$NH$_2$](η^5-C$_5$H$_5$)} (1). Mono-functional **1** was synthesized in two steps from *N*,*N*,*N*-trimethylferrocenylmethyl-ammonium iodide, by adapting the

literature procedures.[9a] 1-Cyanomethylferrocene[44] (5.55 g, 24.4 mmol) in dry diethyl ether (90 mL) was added dropwise to a stirred suspension of $LiAlH_4$ (1.63 g, 43 mmol) in 100 mL of dry diethyl ether and heated at 35 °C. After being stirred for 3 h under reflux, the reaction mixture was externally cooled with an ice bath, and cold water was slowly added dropwise until H_2 release stopped. Once decanted, the solution was acidified by addition of H_2SO_4 6 M. The solid formed was separated by filtration and treated with an 6 N NaOH aqueous solution to adjust the pH to ~11. The dark orange mixture was extracted with diethyl ether, the organic phases were combined, dried (over Na_2CO_3), filtered and the solvent was removed under vacuum. A viscous brown oil was obtained which was dissolved in *n*-hexane and filtered to remove any solid impurities. Solvent removal afforded compound **1** as a viscous oily dark amber-brown product, which can be purified by distillation in vacuum. Yield: 3.7 g (66%). ^{1}H NMR ($CDCl_3$, 300 MHz): δ 1.30 (br, 2H, NH_2), 2.50 (t, ^3J = 7.0 Hz, 2H, Fc–CH_2), 2.80 (t, ^3J = 7.0 Hz, 2H, CH_2–NH_2), 4.07, 4.08 (m, 4H, C_5H_4), 4.10 (s, 5H, C_5H_5). ^{13}C{^{1}H} NMR ($CDCl_3$, 75 MHz): δ 34.1 (Fc–CH_2), 43.6 (CH_2–NH_2), 67.4, 68.4, 86.3 (C_5H_4), 68.6 (C_5H_5). IR (CsI): ν(N–H) 3368, 3292 cm^{-1}, ν(C–H) 3091, 2927, 2853 cm^{-1}, δ(N–H) 1587 cm^{-1}, δ(C–H) 818 cm^{-1}, ρ(Fe–ring) 483 cm^{-1}. MS (FAB$^+$): *m*/*z* 229.1 [M$^+$].

Synthesis of Fe{η^5-$C_5H_4(CH_2)_2NH_2$}$_2$ (2). Bifunctionalized **2** was synthesized in several steps starting from commercially available 1,1′-diacetylferrocene, by adapting the literature procedures. To a room-temperature solution of $LiAlH_4$ (0.82 g, 21.6 mmol) in 34 mL of dry diethyl ether was added dropwise another solution of $AlCl_3$ (2.82 g, 21.2 mmol) in 40 mL of the same solvent. The mixture was treated, dropwise, with a third solution of 1,1′-bis(cyanomethyl)ferrocene[9a] (2.30 g, 8.72 mmol) in 128 mL of diethyl ether. The reaction was refluxed and stirred for 2.5 h. The resulting homogeneous solution was cooled with an external bath and, at the same time, cool water was added dropwise to remove the excess $LiAlH_4$. When no more H_2 was released the addition of water was stopped and a 6 M solution of H_2SO_4 was added to protonate the amine group. The aqueous yellow phase was separated and was brought to pH ~ 11 with a solution of KOH. The aqueous phase was extracted with diethyl ether and the combined organic layers were dried with Na_2CO_3. Filtration and solvent removal afforded compound **2** as a brown oil that was dried in vacuum. Yield: 2.04 g (86%).^{1}H NMR ($CDCl_3$, 300 MHz): δ 1.24 (s, 4H, NH_2), 2.50 (t, ^3J = 6.9 Hz, 4H, Fc–CH_2), 2.80 (t, ^3J = 6.9 Hz, 4H, CH_2–NH_2), 4.01, 4.02 (m, 8H, C_5H_4). ^{13}C{^{1}H} NMR ($CDCl_3$, 75 MHz): δ 33.6 (Fc–CH_2), 43.3 (CH_2–NH_2), 68.2, 69.1, 86.2 (C_5H_4). IR (CsI): ν(N–H) 3358, 3292, cm^{-1}, ν(C–H) 3085, 2922, 2864 cm^{-1}, δ(N–H) 1663 cm^{-1}, δ(C–H) 818 cm^{-1}, ρ(Fe–ring) 489 cm^{-1}. MS (FAB$^+$): *m*/*z* 272.1 [M$^+$].

Synthesis of *cis*-dichloro[1,1′-bis(β-aminoethyl)ferrocene] platinum(II) (3). A solution of **2** (288 mg, 1.06 mmol) in 30 mL of dry dichloromethane was added under argon to another solution of $K_2[PtCl_4]$ (200 mg, 0.482 mmol) in a mixture of 14 mL of distilled water and 7 mL of ethanol. The mixture was stirred at room temperature under argon for 48 h. The solution was concentrated and the solid formed was filtered, washed with cold CH_2Cl_2, H_2O and EtOH and dried under vacuum to give compound **3**. Yield: 105 mg (38%). Elemental analysis (%) calcd. for $C_{14}H_{20}Cl_2FeN_2Pt$: C 31.28, H 3.75, N 5.22; found: C 31.57, H 3.71, N 5.59. IR (KBr): ν(N–H) 3437, 3197 cm^{-1}, ν(C–H) 3080, 2918 cm^{-1}, δ(N–H) 1578 cm^{-1}, δ(C–H) 806 cm^{-1}, ρ(Fe–ring) and ν(Pt–N) 487 cm^{-1}, ν(Pt–Cl) 330, 321 cm^{-1}. MS (ESI$^+$): *m*/*z* 501.0 [M–Cl]$^+$.

Synthesis of *cis*-chloro(dimethylsulfoxide)[1,1′-bis(β-aminoethyl)ferrocene] platinum(II) (4). A solution of **2** (200 mg, 0.74 mmol) in 40 mL of dry CH_2Cl_2 was added, *via* cannula, to a solution of *cis*-[$PtCl_2$(dmso)$_2$] (207.3 mg, 0.491 mmol) in 80 mL of the same solvent. The mixture was stirred at room temperature for 72 h and the resulting solution was concentrated under vacuum until the appearance of an orange solid, which was filtered, washed with CH_2Cl_2 and acetone and dried under vacuum to afford the desired compound 4. Yield: 115 mg (40%). Elemental analysis (%) calcd. for $C_{16}H_{26}ClFeN_2PtSO$: C 33.10, H 4.52, N 4.83, S 5.51; found: C 32.98, H 4.61, N 4.68, S 5.62. ^{1}H NMR ($(CD_3)_2CO$, 300 MHz): δ 2.87 (t, ^3J = 7.5 Hz, 4H, Fc–CH_2), 3.12 (q, ^3J = 7.5 Hz, 4H, CH_2–NH_2), 3.34 (s, $^3J_{Pt\text{-}H}$ = 19.1 Hz, 6H, CH_3), 4.19, 4.12 (m, 8H, C_5H_4), 4.50 (br, 4H, NH_2). ^{13}C{^{1}H} NMR ($(CD_3)_2CO$, 75 MHz): δ 29.7 (Fc–CH_2), 42.8 (CH_3–S), 46.0 (CH_2–NH_2), 68.2, 68.7 (C_5H_4), 85.2 (C_{ipso}). ^{195}Pt NMR ($(CD_3)_2CO$, 64 MHz) δ −3120. IR (KBr): ν(N–H) 3409, 3181 cm^{-1}, ν(C–H) 3074, 2912 cm^{-1}, δ(N–H) 1583 cm^{-1}, ν(S=O) 1124 cm^{-1}, δ(C–H) 805 cm^{-1}, ρ(Fe–ring) and ν(Pt–N) 487 cm^{-1}, ν(Pt–S) 441 cm^{-1}, ν(Pt–Cl) 333 cm^{-1}. MS (ESI$^+$): *m*/*z* 580.0 [M$^+$].

Synthesis of *cis*-dichlorobis[1-β-aminoethylferrocene] platinum(II) (5). A solution of **1** (500.5 mg, 2.18 mmol) in dry CH_2Cl_2 (17 mL) was added, *via* cannula, to another solution of $K_2[PtCl_4]$ (410.0 mg, 0.993 mmol) in a mixture of 17 mL of distilled water and 9 mL of ethanol. The mixture was vigorously stirred at 40 °C for 24 h. After the organic phase was extracted, CH_2Cl_2 was added and the solution was kept at −30 °C for 2 h. The orange solid isolated was separated by filtration, washed with CH_2Cl_2 and dried under vacuum to give compound **5**. Yield: 380 mg (53%). Elemental analysis (%) calcd. for: $C_{24}H_{30}Cl_2Fe_2N_2Pt$: C 39.83, H 4.18, N 3.87; found: C 40.04, H 4.11, N 3.68. ^{1}H NMR (dmso-d_6, 300 MHz): δ 2.63 (m, 4H, Fc–CH_2), 2.82 (m, 4H, CH_2–NH_2), 4.08, 4.13 (m, 8H, C_5H_4), 4.16 (s, 10H, C_5H_5), 4.98 (br, 4H, NH_2). ^{13}C{^{1}H} NMR (dmso-d_6, 75 MHz): δ 30.4 (Fc–CH_2), 47.2 (CH_2–NH_2), 67.6, 68.0 (C_5H_4), 68.8 (C_5H_5), 85.5 (C_{ipso}). ^{195}Pt NMR (dmso-d_6, 64 MHz): δ −2210. IR (KBr): ν(N–H) 3458, 3221 cm^{-1}, ν(C–H) 3136, 2914 cm^{-1}, δ(N–H) 1581 cm^{-1}, δ(C–H) 811 cm^{-1}, ρ(Fe–ring) and ν(Pt–N) 485 cm^{-1}, ν(Pt–Cl) 327, 317 cm^{-1}. MS (ESI$^+$): *m*/*z* 723.0 [M$^+$], 688.0 [M–Cl]$^+$.

Synthesis of *cis*-dichloro(dimethylsulfoxide)(1-β-aminoethyl ferrocene)platinum(II) (6). A solution of **1** (500 mg, 2.18 mmol) in 68 mL of dry CH_2Cl_2 was added, *via* cannula, to a second solution of *cis*-[$PtCl_2$(dmso)$_2$] (459.4 mg, 1.09 mmol) in 110 mL of CH_2Cl_2. The mixture was stirred at room temperature for two days and the resulting solution was concentrated to *ca.* 90 mL and cooled to −30 °C. The orange precipitate formed was filtered off, washed with CH_2Cl_2 and dried under vacuum. The compound was purified by column chromatography on silica gel 60 silanized using AcOEt as eluent to afford compound **6**. Yield: 320 mg (51%). Elemental analysis (%) calcd. for: $C_{14}H_{21}Cl_2FeNPtSO$: C 29.37, H 3.70, N 2.45, S 5.59. Found: C 29.54, H 3.75, N 2.68, S 5.38. ^{1}H NMR (CD_2Cl_2, 300 MHz): δ 2.69 (t, ^3J = 7.0 Hz, 2H, Fc–CH_2), 3.14 (m, 2H, CH_2–NH_2), 3.44 (s, $^3J_{Pt\text{-}H}$ = 25.5 Hz,

6H, CH_3), 3.82 (br, 2H, NH_2), 4.13 (m, 4H, C_5H_4), 4.14 (s, 5H, C_5H_5). $^{13}C\{^1H\}$ NMR (CD_2Cl_2, 125 MHz): δ 31.3 (Fc–CH_2), 44.3 (CH_3–S), 48.4 (CH_2–NH_2), 68.0, 68.2 (C_5H_4), 68.7 (C_5H_5), 83.2 (C_{ipso}). ^{195}Pt NMR (CD_2Cl_2, 107 MHz) δ –3097. IR (KBr): ν(N–H) 3448, 3208 cm^{-1}, ν(C–H) 3092, 2914 cm^{-1}, δ(N–H) 1566 cm^{-1}, ν(S=O) 1123 cm^{-1}, δ(C–H) 817 cm^{-1}, ρ(Fe–ring) and ν(Pt–N) 483 cm^{-1}, ν(Pt–S) 444 cm^{-1}, ν(Pt–Cl) 341, 317 cm^{-1}. MS (ESI$^+$): m/z 594.9 [M+Na]$^+$.

Conclusions

In summary, a family of new electroactive heterometallic compounds containing β-aminoethylferrocenyl moieties and platinum(II) centers has been successfully prepared and characterized. Electrochemical data revealed that all mixed ferrocene–platinum compounds **3–6** undergo one-electron (for **3**, **4** and **6**) or two-electron (for **5**) reversible oxidations, and that in trimetallic **5** the two ferrocenyl redox units are electrochemically independent. *In vitro*, heterometallic monoferrocenyl compounds **4** and **6** do not show considerable cytotoxicity against representative human cancer cell lines. In contrast, trimetallic **5**, bearing two redox-active ethylferrocenyl units linked to the platinum center through NH_2 linkages, is active against all cell lines tested, even in the more resistant colon cancer cell line. Cell cycle studies demonstrate that the new compounds show a different mechanism of action to that of the standard anticancer drug cisplatin. Although the exact biological target remains unknown, ongoing work will shed light on the specific mechanism of action of the new trimetallic compound and its scope as an anticancer drug.

Acknowledgements

We gratefully acknowledge financial support from the Spanish Ministerio de Ciencia e Innovación, Projects CTQ2009-09125/BQU, SAF2009-09431 and CTQ2008-06806-C02-01/BQU, MSC (RTICC RD06/0020/1046), the Canary Islands ACIISI (PI 2007/021) and FUNCIS (PI 43/09). S. B. thanks the Spanish Ministerio de Educación y Ciencia for a FPU grant and L. G. L. thanks the MSC-FIS for an S. Borrell contract.

Notes and references

1 *Ferrocenes: Ligands, Materials and Biomolecules*, ed. P. Stèpnicka, Wiley, UK, 2008.
2 P. Jutzi and T. Redeker, *Eur. J. Inorg. Chem.*, 1998, 663–674.
3 For recent examples of amino-functionalised ferrocenes, see:(*a*) K. M. Joly, B. M. Kariuki, D. M. Coe and L. R. Cox, *Organometallics*, 2005, **24**, 358–366; (*b*) K. M. Joly, R. M. Gleixner, S. M. E. Simpkins, D. M. Coe and L. R. Cox, *Tetrahedron*, 2007, **63**, 761–767; (*c*) K. R. Nikolaides, S. D. Hoffmann and J. Eppinger, *J. Organomet. Chem.*, 2008, **693**, 2223–2230.
4 See for example: (*a*) K. Kavallieratos, S. Hwang and R. H. Crabtree, *Inorg. Chem.*, 1999, **38**, 5184–5186; (*b*) F. Zapata, A. Caballero, A. Tárraga and P. Molina, *J. Org. Chem.*, 2010, **75**, 162–169; (*c*) P. D. Beer and S. R. Bayly, *Top. Curr. Chem.*, 2005, **255**, 125–162 and references cited therein.
5 S. Asaftei and L. Walter, *Electrochim. Acta*, 2004, **49**, 4679–4685.
6 Y. Wu, S. Liu and L. He, *Anal. Chem.*, 2009, **81**, 7015–7021.
7 (*a*) V. C. Gibson, C. K. A. Gregson, C. M. Halliwell, N. J. Long, P. J. Oxford, A. J. P. White and D. J. Williams, *J. Organomet. Chem.*, 2005, **690**, 6271–6283; (*b*) V. C. Gibson, C. M. Halliwell, N. J. Long, P. J. Oxford, A. M. Smith, A. J. P. White and D. J. Williams, *Dalton Trans.*, 2003, 918–926.
8 H.-K. Kim, J.-A. Park, K. M. Kim, Sk. Md. Nasiruzzaman, D.-S. Kang, J. Lee, Y. Chang and T.-J. Kim, *Chem. Commun.*, 2010, **46**, 8442–8444.
9 (*a*) K. E Gonsalves, R. Lenz and M. D. Rausch, *Appl. Organomet. Chem.*, 1987, **1**, 81–93; (*b*) K. E Gonsalves and M. D. Rausch, *J. Polym. Sci., Part A: Polym. Chem.*, 1988, **26**, 2769–2775; (*c*) K. Gonsalves, L. Zhan-Ru and M. D. Rausch, *J. Am. Chem. Soc.*, 1984, **106**, 3862–3863.
10 C. M. Casado, M. Morán, J. Losada and I. Cuadrado, *Inorg. Chem.*, 1995, **34**, 1668–1680.
11 (*a*) I. Cuadrado, M. Morán, J. Losada, C. M. Casado, C. Pascual, B. Alonso and F. Lobete, In *Advances in Dendritic Macromolecules*, G. R. Newkome Ed.; JAI Press, Greenwich, Connecticut, 1996; Vol 3, pp. 151–195; (*b*) I. Cuadrado, M. Morán, C. M. Casado, B. Alonso and J. Losada, *Coord. Chem. Rev.*, 1999, **193–195**, 395–445.
12 C. M. Casado, I. Cuadrado, B. Alonso, M. Morán and J. Losada, *J. Electroanal. Chem.*, 1999, **463**, 87–92.
13 (*a*) R. Bosque and C. López, *Polyhedron*, 1999, **18**, 135–143; (*b*) P. Ramani, R. Ranatunge-Bandarage, B. H. Robinson and J. Simpson, *Organometallics*, 1994, **13**, 500–510.
14 (*a*) G. Jaouen , Ed. *Bioorganometallics: Biomolecules, Labeling, Medicine*, Wiley-VCH, Weinheim, Germany, 2006; (*b*) C. S. Allardyce, P. J. Dyson, *Medicinal Properties of Organometallic Compounds, in Bioorganometallic Chemistry*, ed. G. Simonneaux, Springer, Germany, 2006, vol. 17, ch. 6, pp 177–210; (*c*) E. A. Hillard and G. Jaouen, *Organometallics*, 2011, **30**, 20–27.
15 For excellent recent reviews on the bioorganometallic chemistry of ferrocene-containing compounds, see: (*a*) D. R. van Staveren and N. Metzler-Nolte, *Chem. Rev.*, 2004, **104**, 5931–5985; (*b*) M. F. R. Fouda, M. M. Abd-Elzaher, R. A. Abdelsamaia and A. A. Labib, *Appl. Organomet. Chem.*, 2007, **21**, 613–625; (*c*) R. H. Fish and G. Jaouen, *Organometallics*, 2003, **22**, 2166; (*d*) M. Salmain and N. Metzler-Nolte, *Bioorganometallic Chemistry of Ferrocene*, in *Ferrocenes* ed. P. Stepnicka, John Wiley & Sons, Chichester, U.K., 2008, pp 499-639; (*e*) G. Gasser, I. Ott and N. Metzler-Nolte, *J. Med. Chem.*, 2011, **54**, 3–25.
16 See for example: (*a*) P. Köpf-Maier, H. Köpf and E. W. Neuse, *Angew. Chem., Int. Ed. Engl.*, 1984, **23**, 456–457; (*b*) P. A. Ferreira, J. L. Ferreira da Silva, M. T. Duarte, M. F. Minas da Piedade, M. P. Robalo, S. G. Harjivan, C. Marzano, V. Gandin and M. M. Marques, *Organometallics*, 2009, **28**, 5412–5423; (*c*) E. Hillard, A. Vessières, L. Thouin, G. Jaouen and C. Amatore, *Angew. Chem., Int. Ed.*, 2006, **45**, 285–290; (*d*) G. Jaouen, S. Top, A. Vessières, G. Leclercq and M. J. McGlinchey, *Curr. Med. Chem.*, 2004, **11**, 2505–2517; (*e*) E. Hillard, A. Vessières, F. Le Bideau, D. Plazuk, D. Spera, M. Huche and G. Jaouen, *ChemMedChem*, 2006, **1**, 551–559; (*f*) P. Pigeon, S. Top, A. Vessières, M. Huché, M. Görmen, M. El Arbi, M. Plamont, M. J. McGlinchey and G. Jaouen, *New J. Chem.*, 2011, **35**, 2212; (*g*) M. Gormen, P. Pigeon, S. Top, A. Vessières, M. A. Plamont, E. A. Hillard and G. Jaouen, *Med. Chem. Commun.*, 2010, **1**, 149–151; (*h*) M. Gormen, P. Pigeon, S. Top, E. A. Hillard, M. Huche, C. G. Hartinger, F. de Montigny, M. A. Plamont, A. Vessières and G. Jaouen, *ChemMedChem*, 2010, **5**, 2039–2050.
17 For recent interesting examples of heterometallic ferrocene-platinum compounds, see: (*a*) P. Stepnicka, H. Solarová, M. Lamac and I. Císarová, *J. Organomet. Chem.*, 2010, **695**, 2423–2431; (*b*) E. J. Velazco, A. J. M. Caffyn, X. F. Le Goff and L. Ricard, *Organometallics*, 2008, **27**, 2402–2404; (*c*) A. Dıez, J. Fernandez, E. Lalinde, M. T. Moreno and S. Sanchez, *Inorg. Chem.*, 2010, **49**, 11606–11618; (*d*) K. Heinze and S. Reinhardt, *Organometallics*, 2007, **26**, 5406–5414; (*e*) R. Malacea, L. Routaboul, E. Manoury, J.-C. Daran and R. J. Poli, *J. Organomet. Chem.*, 2008, **693**, 1469–1477; (*f*) R. Packheiser, B. Walfort and H. Lang, *Organometallics*, 2006, **25**, 4579–4587; (*g*) M. M. Dell'Anna, U. Englert, M. Latronico, P. Lorenzo, P. Mastrorilli, D. G. Papa, C. M. Nobile and M. Peruzzin, *Inorg. Chem.*, 2006, **45**, 6892–6900; (*h*) S. Jamali, S. M. Nabavizadeh and M. Rashidi, *Inorg. Chem.*, 2008, **47**, 5441–5452; (*i*) C. L. Mandell, S. S. Kleinbach, W. G. Dougherty, W. S. Kassel and C. Nataro, *Inorg. Chem.*, 2010, **49**, 9718–9727; (*j*) A. Jakob, P. Ecorchard, M. Linseis, R. F. Winter and H. Lang, *J. Organomet. Chem.*, 2009, **694**, 655–666; (*k*) J. Schulz, I. Cisarova and P. Stepnicka, *J. Organomet. Chem.*, 2009, **694**, 2519–2530; (*l*) P. K. Basu, A. Gonzalez, C. Lopez, M. Font-Bardia and T. Calvet, *J. Organomet. Chem.*, 2009, **694**, 3633–3642; (*m*) P. Stepnicka, H. Solarova, M. Lamac and I. Cisarova, *J. Organomet. Chem.*, 2010, **695**, 2423–2431.
18 For recent examples of heterometallic ferrocene–platinum and ferrocene–palladium compounds displaying biological activity, see: (*a*) J. Schulz, A. K. Renfrew, I. Cisarova, P. J. Dyson and P. Stepnicka,

Appl. Organometal. Chem., 2010, **24**, 392–397; (*b*) J. Rajput, J. R. Moss, A. T. Hutton, D. T. Hendricks, C. E. Arendse and C. Imrie, *J. Organomet. Chem.*, 2004, **689**, 1553–1568.
19 For interesting recent examples of mixed ferrocene–ruthenium compounds displaying cytotoxic activity see: M. Auzias, B. Therrien, G. Suess-Fink, P. Stepnicka, W. H. Ang and P. J. Dyson, *Inorg. Chem.*, 2008, **47**, 578–583.
20 I. Cuadrado *Organometallic, Silicon-Containing Dendrimers and their Electrochemical Applications in Silicon-Containing Dendritic Polymers*; ed. P. R. Dvornic and M. J. Owen, Springer, Germany, 2009, vol 2, ch.8, p 141-196.
21 (*a*) S. Bruña, A. M. González-Vadillo, D. Nieto, C. Pastor and I. Cuadrado, *Organometallics*, 2010, **29**, 2796–2807; (*b*) R. Castro, I. Cuadrado, B. Alonso, C. M. Casado, M. Moran and A. E. Kaifer, *J. Am. Chem. Soc.*, 1997, **119**, 5760–5761; (*c*) I. Cuadrado, C. M. Casado, B. Alonso, M. Morán, J. Losada and V. Belsky, *J. Am. Chem. Soc.*, 1997, **119**, 7613–7614; (*d*) B. Alonso, I. Cuadrado, M. Morán and J. Losada, *J. Chem. Soc., Chem. Commun.*, 1994, 2575–2576; (*e*) B. Alonso, C. Casado, I. Cuadrado, M. Morán and A. E. Kaifer, *Chem. Commun.*, 2002, 1778–1779.
22 (*a*) A. M. González-Vadillo, A. Alvarez-Valdés, V. Moneo, F. Blanco, R. G. Díaz, A. Carnero and C. Navarro-Ranninger, *J. Inorg. Biochem.*, 2007, **101**, 551–558; (*b*) E. Montero, S. Diaz, A. M. González-Vadillo, J. M. Pérez, C. Alonso and C. Navarro-Ranninger, *J. Med. Chem.*, 1999, **42**, 4264–4268.
23 D. Nieto, A. M. González-Vadillo, S. Bruña, C. J. Pastor, A. E. Kaifer and I. Cuadrado, *Chem. Commun.*, 2011, **47**, 10398–10400.
24 C. Elschenbroich, *Organometallics*, Wiley-VCH, Weinheim, Germany, 2006.
25 (*a*) A. Ratajczak, B. Czech and L. Drobek, *Synth. React. Inorg. Met.-Org. Chem.*, 1982, **12**, 557–563; (*b*) See also reference 9a.
26 C. U. Pittman Jr., R. L. Voges and W. R. Jones, *Macromolecules*, 1971, **4**, 291–297.
27 E. Pantoja, A. Alvarez-Valdes, J. M. Perez, C. Navarro-Ranninger and J. Reedijk, *Inorg. Chim. Acta*, 2002, **339**, 525–531.
28 A. P. S. Fontes, A. Oskarsson, K. Loevqvist and N. Farrell, *Inorg. Chem.*, 2001, **40**, 1745–1750.
29 (*a*) N. Nedelec and F. D. Rochon, *Inorg. Chim. Acta*, 2001, **319**, 95–108; (*b*) J. Aleman, D. del Solar, A. Álvarez-Vadés, C. Ríos-Luci, J. M. Padrón and C. Navarro-Ranninger, *Med. Chem. Commun.*, 2011, **2**, 789.
30 F. D. Rochon and J. R. L. Priqueler, *Can. J. Chem.*, 2004, **82**, 649–658.
31 F. D. Rochon, C. Bensimon and C. Tessier, *Inorg. Chim. Acta*, 2008, **361**, 16–28.
32 J. B. Flanagan, S. Margel, A. J. Bard and F. C. Anson, *J. Am. Chem. Soc.*, 1978, **100**, 4248–4253.
33 P. O. Miranda, J. M. Padron, J. I. Padron, J. Villar and V. S. Martin, *ChemMedChem*, 2006, **1**, 323–329.
34 A. Monks, D. Scudiero, P. Skehan, R. Shoemaker, K. Paull, D. Vistica, C. Hose, J. Langley, P. Cronise, A. Vaigro-Wolff, M. Gray-Goodrich, H. Campbell and M. R. Mayo, *J. Natl. Cancer Inst.*, 1991, **83**, 757–766.
35 P. E. Pizao, G. J. Peters, J. Van Ark-Otte, L. A. Smets, E. Smitskamp-Wilms, B. Winograd, H. M. Pinedo and G. Giaccone, *Eur. J. Cancer*, 1993, **29A**, 1566–1573.
36 L. G. Leon, R. M. Carballo, M. C. Vega-Hernandez, P. O. Miranda, V. S. Martin, J. I. Padron and J. M. Padron, *ChemMedChem*, 2008, **3**, 1740–1747.
37 J. M. Padron and G. J. Peters, *Invest. New Drugs*, 2006, **24**, 195–202.
38 J. H. Price, A. N. Williamson, R. F. Schramm and B. B. Wayland, *Inorg. Chem.*, 1972, **11**, 1280–1284.
39 G. M. Sheldrick *SADABS Version 2.03*, Program for Empirical Absorption Correction; University of Göttingen: Germany, 1997-2001.
40 *SAINT+NT Version 6.04*; SAX Area-Detector Integration Program; Bruker Analytical X-ray Instruments, Madison, WI, 1997-2001.
41 AXS Bruker. *SHELXTL Version 6.10*, Structure Determination Package; Bruker Analytical X-ray Instruments, Madison, WI, 2000.
42 G. M. Sheldrick, *Acta Crystallogr., Sect. A: Found. Crystallogr.*, 1990, **46**, 467.
43 G. M. Sheldrick *SHELXL97*, Program for Crystal Structure Refinement; University of Göttingen, Germany, 1997 .
44 D. Lednicer and C. R. Hauser, *Organic Syntheses*, 1973, **5**, 578.